Superradiance in ultracold Rydberg gases

T. Wang,[1] S. F. Yelin,[1,2] R. Côté,[1] E. E. Eyler,[1] S. M. Farooqi,[1] P. L. Gould,[1] M. Koštrun,[1,2] D. Tong,[1] and D. Vrinceanu[3]

[1]*Department of Physics, University of Connecticut, Storrs, Connecticut 06269, USA*

[2]*ITAMP, Harvard-Smithsonian Center for Astrophysics, Cambridge, Massachusetts 02138, USA*

[3]*Theoretical Division, Los Alamos National Laboratory, New Mexico 87545, USA*

Experiments in dense, ultracold gases of rubidium Rydberg atoms show a considerable decrease of the radiative excited state lifetimes compared to dilute gases. This accelerated decay is explained by collective and cooperative effects, leading to superradiance. A formalism to calculate effective decay times in a dense Rydberg gas shows that for these atoms the decay into nearby levels increases by up to three orders of magnitude. Excellent agreement between theory and experiment follows from this treatment of Rydberg decay behavior.

In recent years, ultracold atomic gases have been used to probe a variety of many-body phenomena such as Bose-Einstein condensation [1,2] and degenerate Fermi gases [3]. In addition to collective effects due to particle statistics, other manifestations of many-body physics have been explored, such as in slow-light experiments [4] and in ultracold Rydberg gases (e.g., the diffusion of excitations through resonant collisions [5] and the blockade mechanism [6]). Another important fundamental collective effect is superradiance, in which photon exchange between atoms modifies the behavior of the sample. In particular, *cooperative* effects due to virtual photon exchange can lead to the formation of so-called Dicke states [7]. These states are the symmetric superposition of all states with the same total excitation level for constant atom number N. Interest in Dicke states has grown recently because of their potential advantages in quantum information processing [8] and their importance in the behavior of Bose-Einstein condensates [9].

In this paper, we are interested in many-body physics involving photon exchange in an ultracold gas of Rydberg atoms. Because superradiance depends on the atomic density, and because radiative decay of Rydberg atoms takes place predominantly between the closely spaced upper levels, ultracold Rydberg gases are ideal systems to study superradiance. In fact, Rydberg atoms have many interesting properties: their size can become comparable to the atomic separation, and they have huge dipole moments $\wp \sim n^2$, where n is the principal quantum number of the Rydberg state. In addition, for long-wavelength transitions between neighboring Rydberg states of high n the "cooperative parameter" $\mathcal{C} = \mathcal{N}\lambda^3/4\pi^2$ (where $\mathcal{N}$ is the density of atoms, λ is the transition wavelength), is large, which means collective effects are much easier to obtain than for ground-state atoms [10,11]. This was confirmed in earlier experiments for Rydberg atoms at high [12,13] and low temperatures [14]. Note that these many-body effects may pose a limit on the measurement of lifetimes of Rydberg atoms [15] and may cause undesirable frequency shifts in atomic clocks [16].

The source responsible for both virtual and real photon exchange is the dipole-dipole interaction. It governs the build-up as well as the decay of coherence in a dense radiating sample. On the one hand, the virtual exchange of photons is responsible for the so-called exchange interaction. Its strength is exemplified by the energy difference $2\hbar\Omega$

$= \wp^2/2\pi\epsilon_0 r^3$ between the symmetric and antisymmetric single-excitation superposition $|\pm\rangle = (|eg\rangle \pm |ge\rangle)/\sqrt{2}$ of two atoms in their ground g or excited e states separated by r. On the other hand, the real photon exchange is responsible for dephasing of a dense gas and has the same r^{-3} dependence. The interplay of both determines whether the decay speed-up in a dense inverted gas of two-level atoms is mostly incoherent (intensity proportional to atom number N, called "amplified spontaneous emission," ASE) or coherent ($\propto N^2$, called "superradiance" or "superfluorescence"). Experimentally, this difference can be seen in whether there is an initial build-up in the decay intensity, due to the N^2 dependence, or not.

The difficulty of calculating effects including atom-atom cooperation relates to the intractably large number of interconnected degrees of freedom, even if just a few particles are involved. To explore these collective effects, many new ideas, such as the quantum jump approach, were developed to treat superradiance [17–19]. Recently, we successfully incorporated cooperative effects into a formalism for optically dense media. The result is a two-atom master equation for superradiance [20–22]. We apply our model of cooperative radiation build-up to explain the results of an experiment measuring rapid decay of an ultracold Rb Rydberg gas.

The model, as used in Refs. [20,21], is based on perturbation theory carried to second order in the strength of the exchange interaction. Thus, we can eliminate all field and most atomic degrees of freedom which results in an effective two-atom nonlinear equation of motion of the Linblad type,

$$\dot{\rho} = -\frac{1}{2}\sum_{i,j=1,2}\Gamma_{ij}([\rho\sigma_i,\sigma_j^\dagger]+[\sigma_i,\sigma_j^\dagger\rho]) - \frac{1}{2}\sum_{i,j=1,2}(\Gamma_{ij}+\gamma\delta_{ij})$$
$$\times([\rho\sigma_j^\dagger,\sigma_i]+[\sigma_j^\dagger,\sigma_i\rho]),$$

where ρ is a two-atom density operator, $\sigma_i^{(\dagger)}$ is the lowering (raising) operator of the ith atom, γ the spontaneous emission rate, and Γ_{ij} contains the second-order dipole-dipole interaction between atoms i and j. (First-order effects lead to local field effects which do not play a role here [20].) In order to obtain this result, Gaussian (and therefore, classical) light field statistics are assumed, in line with the second-order approximation. In addition, a Markov approximation is

made which is justified if the coherence time of the light fields is shorter than the atomic evolution [29]. Atomic collisions and center-of-mass motion are neglected.

The Γ_{ij} operators can be calculated from $\Gamma_{ij}\delta(t-t')$ $\propto\langle\langle E_i(t)E_j(t')\rangle\rangle$, where E_i denotes the quantum field at the location of atom i, and the cumulant $\langle\langle AB\rangle\rangle\equiv\langle AB\rangle-\langle A\rangle\langle B\rangle$. Γ_{ij}'s contain both the virtual and real photon exchange, and can be calculated for different systems. They can be expressed only as highly nonlinear and implicit functions of the atomic variables ρ [Eqs. (2)]. For small enough probe diameters d retardation effects can be neglected. This approximation is justified in our case because the time it takes for light to propagate through the sample ($\sim 10^{-10}$ s) is significantly shorter than any other time in the system, in particular, the atomic build-up time. Note that sample sizes less than the cubic wavelength, as needed in the Dicke model [7] are not necessary. Thus we can set $\Gamma_{ii}\equiv\Gamma$ and $\Gamma_{ij\neq i}\equiv\bar{\Gamma}$ and simplify Eq. (1),

$$\dot{\rho}_{ee}=-(2\Gamma+\gamma)\rho_{ee}+\Gamma, \tag{1a}$$

$$\dot{m}=-2(2\Gamma+\gamma)m-2\gamma(2\rho_{ee}-1)+8\bar{\Gamma}\rho_{egge}, \tag{1b}$$

$$\dot{\rho}_{egge}=-(2\Gamma+\gamma)\rho_{egge}+\bar{\Gamma}m. \tag{1c}$$

The upper-level population is ρ_{ee}, the inversion product $m=(\rho_{ee}-\rho_{gg})^2$, and the two-atom nondiagonal coupling $\rho_{egge}=\mathrm{Tr}\,\rho|eg\rangle\langle ge|$. (Setting $\rho_{egge}=0$ would lead to the usual single-atom formalism.) In addition, we use

$$\Gamma=\gamma\frac{\rho_{ee}}{2\rho_{ee}-1}(e^{2\zeta}-1)+2\gamma\mathcal{C}^2\varrho^4\frac{\gamma}{\Gamma+\gamma/2}\rho_{egge}I(\zeta,\varrho),$$

$$\bar{\Gamma}=3\gamma\mathcal{C}\varrho\frac{\gamma}{\Gamma+\gamma/2}\rho_{ee}I(\zeta,\varrho)+2\gamma\mathcal{C}^2\varrho^4\frac{\gamma}{\Gamma+\gamma/2}\rho_{egge}I(\zeta,\varrho),$$
$$\tag{2}$$

where

$$\zeta=\frac{1}{2}\mathcal{C}\varrho\frac{\gamma}{\Gamma+\gamma/2}(2\rho_{ee}-1),\quad I(\zeta,\varrho)=\left|\frac{e^{\xi}(1-\xi)+1}{\xi^2}\right|^2_{\xi=\zeta+i\varrho}.$$

The sample size $\varrho=\pi d/\lambda$ is measured relative to the wavelength of the light.

In our initial experiment, we have studied the decay of high-n states using a simple detection scheme with only limited state specificity. First, Rb atoms were trapped and cooled to 100 μK. Next, they were selectively excited by a pulsed UV laser to the 40p state. After a delay time τ, all atoms in states with principal quantum numbers $n\geq 27$ were Stark ionized. The remaining experimental details are the same as in Ref. [23]. As depicted in Fig. 1, the number of ultracold atoms in Rydberg states with $n\geq 27$ decays fast, an estimated 100 times faster than expected in vacuum [30]. We find that this speed-up can be explained by the presence of superradiance and, on some transitions, ASE [12,13,24]. (Alternative explanations for the strength of the speed-up would include so-called avalanche plasma formation [25], where a large fraction of the initial Rydberg atoms would be ionized. How-
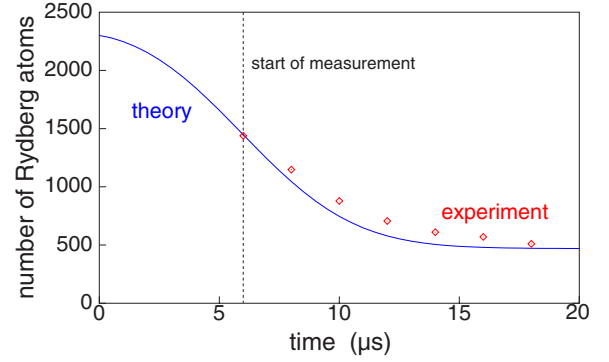

FIG. 1. (Color online) Measured and calculated decay of the number of atoms in Rydberg states with $n\geq 27$ following excitation to $n=43p$. The initial density of Rydberg atoms in the experiment is 5×10^8 cm^{-3}. The dots are experimental points with the vertical dashed line showing the start of experimental measurements, and the solid line theoretical simulation. The fitting parameter in this calculation was the number of atoms present at the start of the measurement, i.e., 1400 Rydberg atoms at 6 μs.

ever, we rule this out because we measure only 190 free ions after a delay of 35 μs.)

In what follows, we will show that Eqs. (1) lead to excellent agreement with the experiment (see Fig. 1). The density in the calculation is chosen to be the same as in the experiment, 5×10^8 cm^{-3}. The sample in the experiment is cigar shaped, thus enabling good mode selection (as in all superradiance experiments to date). In the calculation we make the approximation of having, for each transition, only one mode, and then use, for calculational ease, a spherical geometry with the same sample volume as in the experiment.

The simulations presented here assume Rb atoms in the initial state 40p, exemplifying a range of possible initial states, such as 43p. In Fig. 2 we show the decay from 40p into ns. Similar results are obtained for transitions between P and D states. In Fig. 3, the effective decay times are compared for a dense gas and a vacuum (cf. Ref. [26]). In vacuum, the effective decay time τ_{eff} is the inverse of the
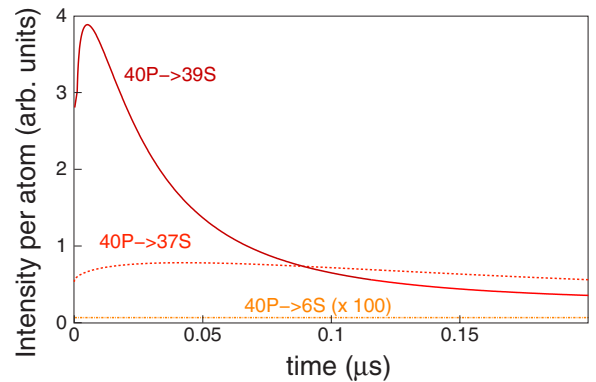

FIG. 2. (Color online) Calculated output intensity as function of time for a sample with density 5×10^8 cm^{-3} for the transition from state 40p to 39s, 37s, and 6s, respectively. The initial increase in intensity over time is the sign for superradiance, i.e., the decay into 39s and 37s qualifies as superradiant, whereas the (very nearly exponential) decay into 6s does not.
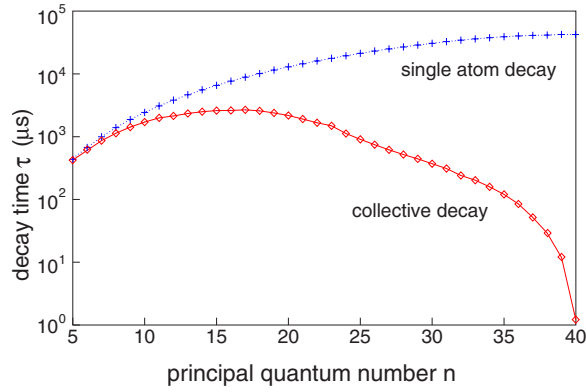
FIG. 3. (Color online) Decay times from $40P$ into various nS states ($\diamond$) in a dense gas ($\mathcal{N}=5\times10^8$ cm^{-3}) and in vacuum (+). The decay times from $40P$ into the corresponding nD states are nearly the same and are therefore not shown.

FIG. 4. (Color online) Map of critical parameters of $\mathcal{C}$ and ϱ (solid line). Above the critical curve (shaded area) are the parameters for which superradiance happens. Also shown are the $\mathcal{C}$ and ϱ for the decay to ns states from $40p$ state (+). Density of atoms is the same as above.

Einstein A-coefficient. Clearly, in a vacuum the transition into the states with lowest n is fastest, and therefore decay into these channels is by far the most likely. But this tendency is reversed dramatically in dense gases: the effective decay time for each transition is shorter by up to three orders of magnitude than that in a vacuum or in dilute gases. Since the collective and cooperative effects responsible for this speed-up depend only on the density relative to the wavelength cubed, the acceleration of the decay is obviously stronger for longer wavelengths. Figure 3 and the quantitative form of the increase in decay for higher densities, particularly for low frequencies, are one of the main results presented in this paper.

It is important at this point to clarify the relative strength and importance of black-body radiation. Black-body radiation, consisting of the thermal photons of a certain wavelength at a certain temperature, competes with the buildup of (coherent) superradiance. Qualitatively, we can estimate that black-body radiation should be important only for $N \ll n_B$, where N is the number of atoms and n_B is the average number of black-body photons per mode at the transition frequency [27]. For the longest-wavelength transition we are studying in the context of this paper, n_B is of the order of only 300, which is considerably less than the photons emitted because of the collectively enhanced rates. We also did a quantitative study where we compare the strength of black-body radiation to the data shown in Fig. 3. The rates are so small that they differ only up to 2% from the bare rates, and are therefore not plotted. (Obviously, the presence of black-body radiation would also increase the collective decay, but here also the effect is so small as to be negligible.)

In Fig. 2, the intensity of some selective decays is shown over time. Because of energy conservation, the intensity must be proportional to the negative time derivative of the upper state population. (We neglect here all time-delay effects, resulting in an instantaneous intensity at time $t=0$.) In this graph, our (somewhat arbitrary) distinction between ASE and superradiance can be seen: An initially positive slope of intensity over time, as seen for $40p \rightarrow 39s$ is associated with superradiance, whereas a monotonically decreasing intensity, as seen for $40p \rightarrow 6s$ means ASE. It is important to
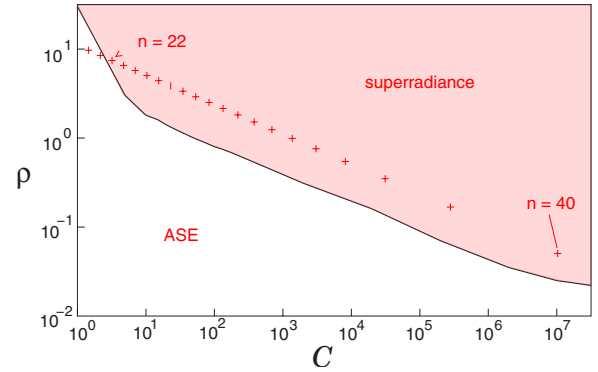
emphasize here again that in reality there is no sharp boundary as there are coherent and incoherent elements mixed in all decays, thus making the transition between the two cases very smooth.

In order to get a general overview of which combination of parameters leads to superradiance, we created a map in the $\mathcal{C}$-ϱ parameter space with relative density or cooperative parameter $\mathcal{C}$ and relative size ϱ. Figure 4 shows the numerically determined border, as defined above, between superradiant and ASE behavior. The selective decay from the $40p$ Rydberg state of Rb into all possible lower ns states is added to the map. We see that superradiant behavior is expected for decay into levels with $n \geq 22$.

We discuss now the calculation shown in Fig. 1. Theoretically, we can calculate, from the decay times as presented in Fig. 3, the lifetime of $40p$ (and the lower states) directly,

$$\frac{1}{\tau_{\text{total}}} = \sum_{\text{all channels out of } 40p} \frac{1}{\tau_{\text{eff}}},$$

and we find $\tau_{\text{total}} \approx 5$ μs. This is to be compared to a $\tau_{\text{total}}^{(0)} = 210$ μs for dilute gas or vacuum. The experiment, however, cannot measure this time directly but only the total lifetime of all states with $n \geq 27$. In order to compare our theoretical method with the experiment we simulate a cascade from $40p$ via all intermediate states down to $n < 27$, using the decay times in Fig. 3 and analogous times for the p, d, f, etc., states with $5 \leq n \leq 40$. This procedure is approximated by using only the two fastest channels out of each state. Numerically, we can compare this result with one that uses one channel more per state and find only small changes of 1%–10%. The result is depicted in the strong black curve in Fig. 1, which shows excellent agreement with the experiment.

Future experiments with improved state-selective detection will allow direct comparison to the single-lifetime calculations.

In this paper, we have discussed the possibility of superradiant decay in cold gases of Rydberg atoms at densities of 10^8–10^9 cm^{-3}. Superradiance occurs because lower-frequency decays are increasingly more likely to happen in

denser gases, and they contribute most to cooperative behavior. Level shifts due to atomic interactions may inhibit superradiance at higher densities and/or higher n. This could explain why superradiance is not routinely seen.

The possibility of mode competition and interference between different decay channels is neglected for simplification. In future work, the effects of geometry, in particular the aspect ratio of the sample, should be taken into account. In practice, only elongated samples are used to show superradiance [28].

Using our calculation we were able to obtain close agreement with observed signatures of superradiance including the effects of dissipation and the unique temporal build-up of a sharp flash of radiation. Moreover, our new formalism allows for easy incorporation of more complicated level structures, additional fields, and polarization effects.

In summary, recent experiments measuring the decay of ultracold Rb Rydberg atoms find rates much faster than that of atoms in dilute gases. These results are consistent with superradiant behavior in the framework of our model.

[1] M. H. Anderson, J. R. Ensher, M. R. Matthrews, C. E. Wieman, and E. A. Cornell, Science **269**, 198 (1995).

[2] K. B. Davis, M.-O. Mewes, M. R. Andrews, N. J. van Druten, D. S. Durfee, D. M. Kurn, and W. Ketterle, Phys. Rev. Lett. **75**, 3969 (1995).

[3] C. A. Regal, M. Greiner, and D. S. Jin, Phys. Rev. Lett. **92**, 040403 (2004).

[4] C. Liu, Z. Dutton, C. H. Behroozi, and L. V. Hau, Nature (London) **409**, 490 (2001).

[5] I. Mourachko, D. Comparat, F. de Tomasi, A. Fioretti, P. Nosbaum, V. M. Akulin, and P. Pillet, Phys. Rev. Lett. **80**, 253 (1998).

[6] D. Tong, S. M. Farooqi, J. Stanojevic, S. Krishnan, Y. P. Zhang, R. Côté, E. E. Eyler, and P. L. Gould, Phys. Rev. Lett. **93**, 063001 (2004).

[7] R. Dicke, Phys. Rev. **93**, 99 (1953).

[8] J. M. Taylor, A. Imamoğlu, and M. D. Lukin, Phys. Rev. Lett. **91**, 246802 (2003).

[9] S. Inouye, A. P. Chikkatur, D. M. Stamper-Kurn, J. Stenger, D. E. Pritchard, and W. Ketterle, Science **285**, 571 (1999).

[10] F. F. Arecchi and E. Courtens, Phys. Rev. A **2**, 1730 (1970).

[11] G. P. Hildred, R. R. Puri, S. S. Hassan, and R. K. Bullough, J. Phys. B **17**, 535 (1984).

[12] F. Gounand, M. Hugon, P. R. Fournier, and J. Berlande, J. Phys. B **12**, 547 (1979).

[13] Y. Kaluzny, P. Goy, M. Gross, J. M. Raimond, and S. Haroche, Phys. Rev. Lett. **51**, 1175 (1983).

[14] B. Barrett, E. Paradis, A. Kumarakrishnan, and G. Raithel, poster JWD 30 at OSA meeting 2006.

[15] A. L. de Oliveira, M. W. Mancini, V. S. Bagnato, and L. G. Marcassa, Phys. Rev. A **65**, 031401(R) (2002).

[16] D. E. Chang, J. Ye, and M. D. Lukin, Phys. Rev. A **69**, 023810 (2004).

[17] J. P. Clemens and H. J. Carmichael, Phys. Rev. A **65**, 023815 (2002).

[18] J. P. Clemens, L. Horvath, B. C. Sanders, and H. J. Carmichael, Phys. Rev. A **68**, 023809 (2003).

[19] J. P. Clemens, L. Horvath, B. C. Sanders, and H. J. Carmichael, J. Opt. B: Quantum Semiclassical Opt. **6**, 736 (2004).

[20] S. F. Yelin, M. Koštrun, T. Wang, and M. Fleischhauer, e-print quant-ph/0509184.

[21] M. Fleischhauer and S. F. Yelin, Phys. Rev. A **59**, 2427 (1999).

[22] S. F. Yelin and M. Fleischhauer, Opt. Express **1**, 160 (1997).

[23] S. M. Farooqi, D. Tong, S. Krishnan, J. Stanojevic, Y. P. Zhang, J. R. Ensher, A. S. Estrin, C. Boisseau, R. Côté, E. E. Eyler *et al.*, Phys. Rev. Lett. **91**, 183002 (2003).

[24] M. Trache, Opt. Commun. **79**, 99 (1990).

[25] M. P. Robinson, B. Laburthe Tolra, M. W. Noel, T. F. Gallagher, and P. Pillet, Phys. Rev. Lett. **85**, 4466 (2000).

[26] M. R. Flannery and D. Vrinceanu, Phys. Rev. A **68**, 030502(R) (2003).

[27] J. M. Raimond, P. Goy, M. Gross, C. Fabre, and S. Haroche, Phys. Rev. Lett. **49**, 1924 (1982).

[28] M. Gross and S. Haroche, Phys. Rep. **93**, 301 (1982).

[29] This Markov approximation is justified self-consistently: the times for atomic and field evolution are compared in the result of the calculation. Although for the fastest evolution times it is not strictly correct to assume atomic evolution to be much slower than field evolution, the approximation is still expected to show good qualitative results. Quantitative estimates of the validity of this procedure will be presented in an upcoming paper.

[30] This factor is a conservative estimate at this time, and it will be quantified more exactly in an improved experimental setting.